NEUROSCIENCE

Autism-like atypical face processing in *Shank3* mutant dogs

Siqi Yuan[1,2], Chenyu Pang[3], Liang Wu[1,2], Li Yi[3], Kun Guo[4], Yong-hui Jiang[5], Yong Q. Zhang[1,2,6]*, Shihui Han[3]*

Atypical face processing is a neurocognitive basis of social deficits in autism spectrum disorder (ASD) and a candidate cognitive marker for the disease. Although hundreds of risk genes have been identified in ASD, it remains unclear whether mutations in a specific gene may cause ASD-like atypical face processing. Dogs have acquired exquisite face processing abilities during domestication and may serve as an effective animal model for studying genetic associations of ASD-like atypical face processing. Here, we showed that dogs with *Shank3* mutations exhibited behavioral and attentional avoidance of faces, contrasting with wild-type controls. Moreover, neural responses specific to faces (versus objects) recorded from the electrodes over the temporal cortex were significantly decreased and delayed in *Shank3* mutants compared to wild-type controls. Cortical responses in the frontal/parietal region underlying categorization of faces by species/breeds were reduced in *Shank3* mutants. Our findings of atypical face processing in dogs with *Shank3* mutations provide a useful animal model for studying ASD mechanisms and treatments.

INTRODUCTION

Autism spectrum disorder (ASD) is a group of neurodevelopmental disorders with impaired social interactions and repetitive behaviors (*1*). A key cognitive basis of social dysfunction in ASD is atypical face processing that is characterized by difficulties in face recognition (*2*), avoidance of eye contact with others (*3*), and impaired structure and function of the neural network involved in face processing (*4*, *5*). ASD is highly heritable with hundreds of risk genes identified (*6*–*8*). Similarly, face cognition (*9*, *10*) and face preference (*11*) have also been shown to have a genetic basis. However, whether mutations in a specific risk gene cause ASD-like atypical face processing remains unclear.

Given the replicated findings of *SHANK3* mutations in patients with ASD (*7*, *12*), animal models with mutations of this gene have been created to examine potential social impairments in ASD. Mouse models with *Shank3* gene mutations showed deficits in social motivation (*13*), social recognition (*14*), and social communication (*15*). *SHANK3* mutant monkeys also exhibited impaired social interactions and increased repetitive behaviors (*16*, *17*). However, none of these animal models have recapitulated the atypical face processing in patients with ASD, limiting our understanding of the genetic link for the abnormal neurocognitive mechanisms underlying face processing in ASD. Specifically, rodents primarily rely on olfactory and whisker-tactile sensory information rather than visual (facial) information during social interactions (*18*).

The present study investigated whether dogs with *Shank3* mutations generated using the CRISPR-Cas9 editing technique (*19*) would show ASD-like deficits in face processing. Domestic dogs (*Canis familiaris*) engage in intimate and complex social interactions with both conspecifics and humans. They can read facial information about individual human identity (i.e., familiar versus unfamiliar faces) (*20*, *21*) and modulate their behaviors in accordance with human social cues (*22*). Dogs exhibit eye contact and gaze-following behavior during interactions with humans (*23*). They also show distinct neural responses to faces versus objects and to faces of conspecifics versus humans in the temporal and parietal cortices (*24*, *25*). These findings indicate dogs as a potential animal model for the investigation of face processing.

Recent studies have revealed social behavior deficits and abnormal auditory responses in *Shank3* mutant dogs that expressed reduced levels of Shank3 isoforms (*19*, *26*). In the present study, we analyzed multimodal measures, including behavioral, eye-tracking, and electrocorticogram (ECoG) measures, to examine possible face processing deficits in *Shank3* mutant dogs. We adapted the experimental paradigms used in studies of human face perception (*27*–*29*) to quantitatively compare behavioral preferences, eye gaze patterns, and ECoG signals in response to face stimuli in wild-type (WT) and *Shank3* mutant dogs. Perceptual discriminations of faces versus nonface objects and faces of different species or breeds are two different levels of face processing that engage distinct neural circuits in both humans (*27*) and dogs (*24*, *25*). We thus investigated whether and how *Shank3* mutations in dogs would affect these two levels of face processing by analyzing behavioral, eye gaze, and ECoG data. Our findings provide consistent evidence for ASD-like atypical face processing in *Shank3* mutant dogs that provide a valid animal model for understanding the neurocognitive mechanisms of ASD and developing interventions for the disease.

RESULTS

Behavioral avoidance for faces in *Shank3* mutants

Behavioral preferences for faces as an index of motivations for sociality have been documented in humans and other animals including dogs (*30*–*32*). We therefore examined whether WT dogs showed

[1]State Key Laboratory for Molecular and Developmental Biology, Institute of Genetics and Developmental Biology, Chinese Academy of Sciences, Beijing, China. [2]University of the Chinese Academy of Sciences, Beijing, China. [3]School of Psychological and Cognitive Sciences, PKU-IDG/McGovern Institute for Brain Research, Peking University, Beijing, China. [4]School of Psychology, University of Lincoln, Brayford Pool, Lincoln LN6 7TS, UK. [5]Department of Genetics and Neuroscience, Yale University School of Medicine, New Haven, CT 06510, USA. [6]School of Life Sciences, Hubei University, Wuhan 430415, China.
*Corresponding author. Email: shan@pku.edu.cn (S.H.); yqzhang@genetics.ac.cn (Y.Q.Z.)

spontaneous behavioral preferences for faces over nonface objects and whether such preferences would be changed because of *Shank3* mutations. We examined behavioral preferences for faces of WT controls and *Shank3* mutants (all beagles; see Materials and Methods and tables S1 and S2 for details) using an approach-avoidance test modified from a previous study (*33*). During the test, a food tray was placed at the bottom of each of the two computer monitors separated by a board (Fig. 1A). At the beginning of each trial, identical dog snacks were placed on each of the two trays. Two black-and-white photos of a beagle face and a house were displayed simultaneously side by side on the two monitors, and their left and right positions varied randomly across trials (Fig. 1B). A test dog was guided to sit in the middle of the testing room facing the monitors for 3 to 5 s before being released to approach one of the two sides. Behavioral preferences for faces were quantified as the percentage of trials in which a dog approached the face.

The results showed that WT controls approached faces significantly more often than the chance level of 50% [65.2 ± 2.55% (mean ± SEM), $t(15) = 5.988$, $P < 0.001$; Fig. 1B]. *Shank3* mutants, however, approached faces less frequently (i.e., approached houses more frequently) than the chance level [38.8 ± 2.64%, $t(13) = 4.235$, $P = 0.001$]. Thus, WT controls and *Shank3* mutants showed opposite patterns of behavioral responses in the approach-avoidance test. Face and house stimuli were different in both low-level visual features (e.g., contrast and spatial frequency) and high-level perceptual category. To test whether the distinct behavioral responses observed in WT and *Shank3* mutants were caused by different low-level visual features or high-level perceptual categories of the stimuli, we conducted the approach-avoidance test using faces and houses that were presented upside down. Low-level visual features were the same for inverted and upright face and house stimuli, whereas perceptual categorization of inverted faces and houses was deteriorated (*34*, *35*). The results showed that neither WT controls nor *Shank3* mutants approached inverted faces at an above-chance level (WT, 54.2 ± 2.70%, $P = 0.176$; mutants, 50.6 ± 2.30%, $P = 0.973$; Fig. 1C), indicating negligible contribution of low-level visual features of the visual stimuli to the distinct behavioral preferences to faces and houses in WT and *Shank3* mutants.

To exclude the possibility that houses rather than faces produced the distinct patterns of behavioral responses to face and house stimuli, we tested WT controls and *Shank3* mutants in the approach-avoidance test using black-and-white photos of houses and cars as paired stimuli. The results showed that neither WT controls nor *Shank3* mutants approached houses at an above-chance level (WT, 48.4 ± 3.28%, $P = 0.766$; mutants, 50.6 ± 2.59%, $P = 0.938$; Fig. 1D), providing no evidence that houses induced any behavioral preference or avoidance in either WT or mutant dogs. Together, these results demonstrated behavioral preferences for faces in WT controls but behavioral avoidance of faces in *Shank3* mutants.

Reduced attention to faces in *Shank3* mutants

Next, we used a human eye-tracking paradigm to examine whether the lack of behavioral preferences for faces in *Shank3* mutants was accompanied by impaired attention to face stimuli, similar to the findings in children with ASD (*28*, *36*). We analyzed eye gazes when WT controls and mutants viewed paired photos of a face and a house that were simultaneously displayed for 3 s (Fig. 2A). WT controls and mutants showed distinct heatmaps of gaze distributions when viewing the stimuli in Fig. 2B. We then quantified visual attention to faces

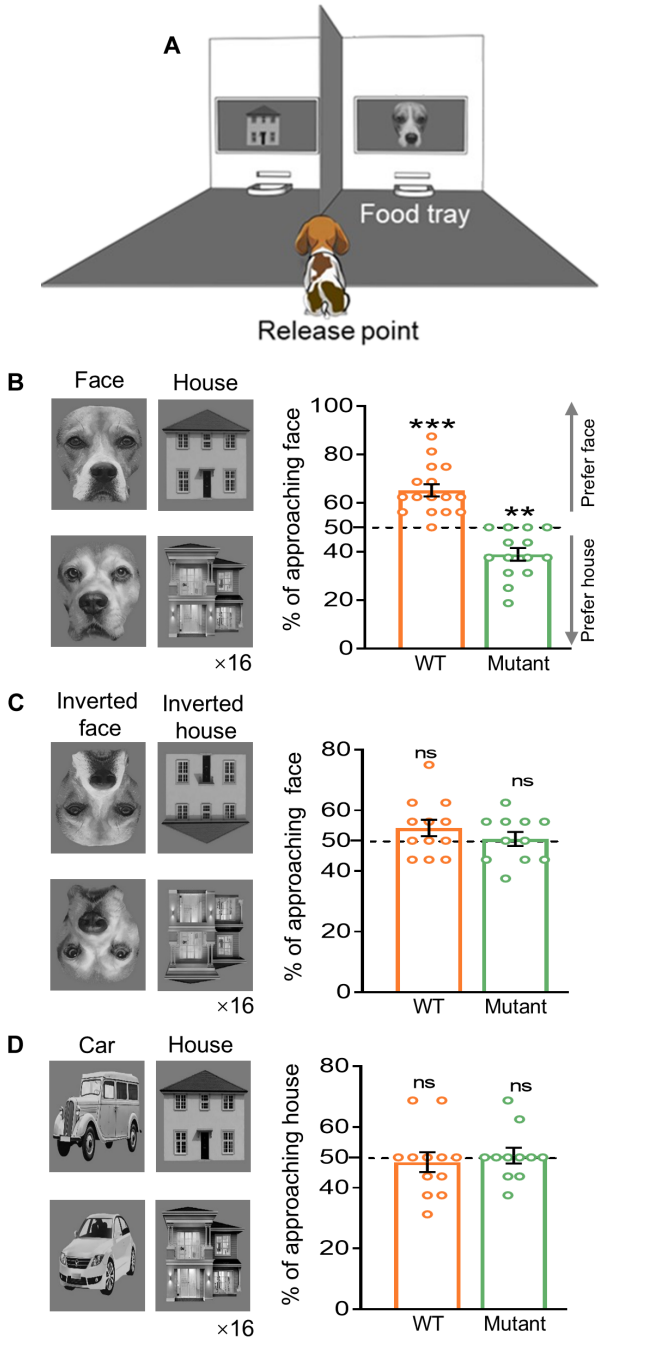

Fig. 1. Behavioral preference for nonface over face stimuli in *Shank3* mutant dogs. (**A**) Illustration of the approach-avoidance test. In each trial, a dog was guided to sit in the middle of the testing room facing the monitors and 2.4 m away from the screen for 3 to 5 s and then released to make a choice. (**B**) The left panel shows two examples of the upright beagle face versus house pairs. Each photo of 20.3 cm by 25.4 cm was displayed in the center of a 23.7-inch (60.198-cm) monitor. The right panel shows the mean percentage of approaching faces in WT ($n = 16$) and mutant dogs ($n = 12$). (**C**) Two examples of the inverted beagle versus house pairs (left). The mean percentage of approaching inverted faces in WT ($n = 12$) and mutant dogs ($n = 11$) (right). (**D**) Two examples of the upright car versus house pairs (left). The mean percentage of approaching house in WT ($n = 12$) and mutant dogs ($n = 11$) (right). Data are presented as means ± SEM. The colored circles represent the data points of individual animals. $^{**}P < 0.01$; $^{***}P < 0.001$; ns, not significant.

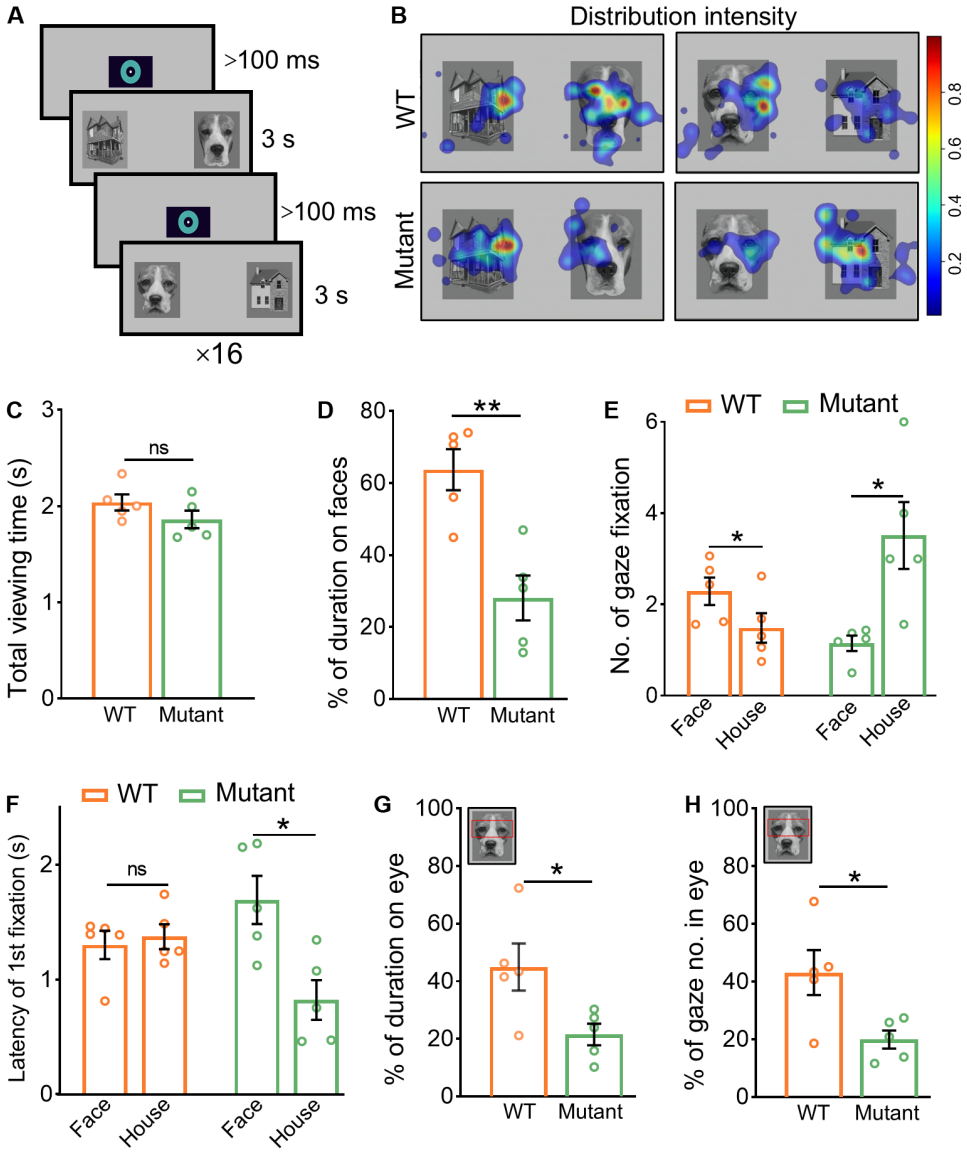

Fig. 2. Eye gaze biases toward nonface over face stimuli in *Shank3* mutant dogs. (**A**) A schematic diagram of the eye-tracking procedure. (**B**) Heatmaps of fixation durations in representative WT and mutants. The scale indicates fixation distribution intensity. A warmer color in the heatmap indicates a longer fixation duration. (**C**) Total viewing time on screen by WT ($n = 5$) and mutant dogs ($n = 5$). (**D**) The mean percentage of fixation durations on faces. One-sample *t* test was used. (**E**) The mean number of fixations. (**F**) The mean latency of the first fixation at face or house stimuli. (**G**) The mean percentage of durations of gaze at the eye region (versus faces) in WT and *Shank3* mutant dogs. (**H**) The mean percentage of numbers of fixations at the eye region (versus faces) in WT and *Shank3* mutant dogs. Data are presented as means ± SEM. The colored circles represent the data points of individual animals. *$P < 0.05$; **$P < 0.01$; ns, not significant.

or houses by analyzing fixation durations, numbers of gaze fixations, and latencies of the first fixation to faces and houses. To test whether *Shank3* mutants compared to WT controls paid less attention to face stimuli, we conducted individual-based statistical analyses to compare the eye-tracking data in the two testing groups. We found that, while WT controls and mutants showed similar total time of viewing the screen (2.0 ± 0.08 s versus 1.9 ± 0.09 s, nonparametric Mann-Whitney tests, $U = 6$, $P = 0.111$; Fig. 2C), WT controls fixated on face stimuli significantly longer than *Shank3* mutants (63.7 ± 5.70 s versus 28.1 ± 6.23 s, $U = 1$, $P = 0.008$; Fig. 2D). Moreover, WT controls showed more gaze fixations on faces than on houses (nonparametric Wilcoxon matched-pairs signed-rank tests, $Z = -2.023$, $P = 0.031$), whereas *Shank3* mutants showed more gaze fixations on houses than on faces ($Z = -2.023$, $P = 0.031$; Fig. 2E). We also analyzed the first fixation latency and found that *Shank3* mutants moved gazes faster to houses than to faces, whereas no such difference was observed in WT (WT controls, $Z = -0.674$, $P = 0.313$; *Shank3* mutants, $Z = -2.023$, $P = 0.031$; Fig. 2F). These results together revealed an attentional bias to faces in WT controls but reduced attention to faces in *Shank3* mutants.

Because reduced attention to the eye region in faces is a prominent feature among patients with ASD (*37*), we further analyzed the patterns of gaze movements in the eye region of the face stimuli. In comparison with WT dogs, *Shank3* mutants exhibited a shorter duration

of gaze (44.9 ± 8.16% versus 21.5 ± 3.72%, $U = 3$, $P = 0.028$; Fig. 2G) and fewer fixations in the eye region (43.1 ± 7.80% versus 19.9 ± 3.15%, $U = 3$, $P = 0.028$; Fig. 2H). Thus, contrary to the attentional bias toward faces in WT controls, *Shank3* mutants show an attentional bias toward nonface stimuli and toward noneye regions of faces, recapitulating impaired attention to faces in children with ASD (*37*, *38*).

Decreased and delayed N1 cortical responses specific to faces in *Shank3* mutants

The distinct patterns of behavioral preferences and attention biases toward faces versus houses in WT and *Shank3* mutants imply altered neural underpinnings of face processing due to *Shank3* mutation. We tested this possibility by recording ECoG signals evoked by face (dog and human faces) and nonface (houses) stimuli in WT and mutant animals. Given the greater neural sensitivity to faces in the right than in the left hemisphere (*39*), ECoG signals were recorded from 32 electrodes over the right frontal, parietal, temporal, and occipital cortices as previously reported (fig. S2) (*26*). Visual stimuli elicit event-related potentials (ERPs) in most brain regions (fig. S3). We statistically analyzed signals from the temporal electrodes that showed the largest difference in ERPs elicited by faces and houses (see below), while the ECoG signals from the frontal/parietal regions did not show significant differences in the amplitudes or latencies specific to faces between WT and mutants (fig. S4). ERPs in response to faces and houses at the temporal electrodes included an early positive activity (P1; peaking at 43 to 66 ms after stimulus onset), a following negative activity (N1; 89 to 123 ms), and a late positive activity (P2; 212 to 263 ms) (Fig. 3, A and B, and table S3).

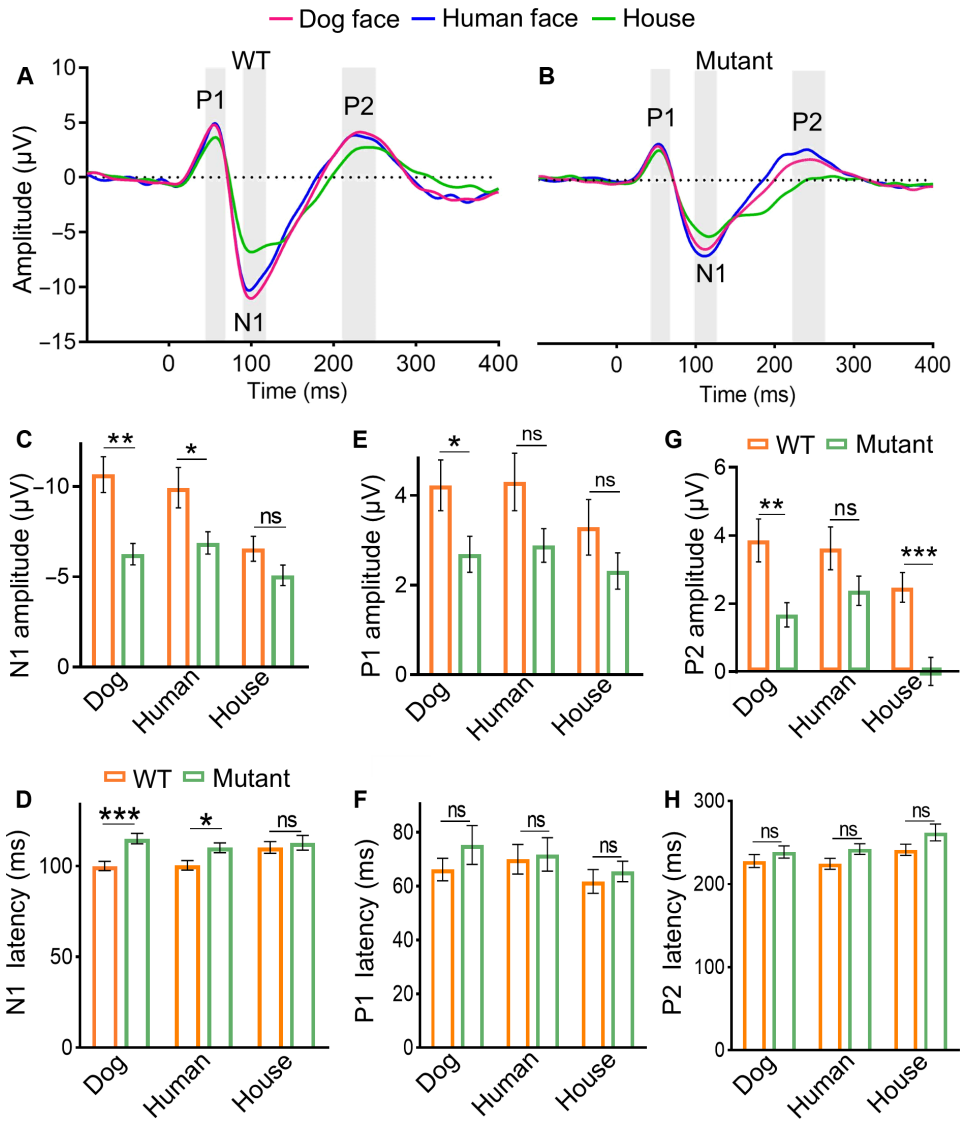

Fig. 3. Decreased and delayed face-specific/N1 responses in *Shank3* mutant dogs. (**A** and **B**) ERPs to dog faces, human faces, and houses recorded at the temporal electrodes in WT ($n = 5$) and *Shank3* mutant dogs ($n = 5$). The gray bar indicates the time windows used for calculating the mean amplitudes of P1, N1, and P2 amplitudes. (**C**, **E**, and **G**) The mean N1 (C), P1 (E), and P2 (G) amplitudes to face and house stimuli in WT and *Shank3* mutant dogs. (**D**, **F**, and **H**) The mean N1 (D), P1 (F), and P2 (H) peak latencies to face and house stimuli in WT and *Shank3* mutant dogs. The notation of significance on the graph refers to the results of ANOVA. Data are presented as means ± SEM. *$P < 0.05$; **$P < 0.01$; ***$P < 0.001$; ns, not significant.

To quantitatively compare neural responses specific to faces between WT controls and *Shank3* mutants, we conducted repeated-measures analyses of variance (ANOVAs) of the mean P1/N1/P2 amplitudes with *stimulus category* (human face versus dog face versus house) as a within-subjects factor and *testing group* (WT versus *Shank3* mutants) as a between-subjects factor. We also conducted linear mixed-effect model (LMM) analyses of the ERP amplitudes using the mixed-effect single-trial regression models to account for potential effects of within-subject correlations. The LMM analyses were not applied to the peak latencies that were not able to be extracted from a single trial. The results of statistical analyses of the ERP amplitudes revealed a significant main effect of stimulus category on N1 amplitudes [$F(2,96) = 41.622$, $P < 0.001$; LMM results, $F(2,14,029) = 59.514$, $P < 0.001$; Fig. 3C and table S4], suggesting greater N1 responses to dog/human faces than houses. This effect, however, was reduced in *Shank3* mutants compared to WT as indicated by a significant *stimulus category* × *testing group* interaction on the N1 amplitudes [$F(2,96) = 9.856$, $P < 0.001$; LMM results, $F(2,14,029) = 12.474$, $P < 0.001$] that indicated decreased face-specific N1 response in *Shank3* mutants. Further comparisons revealed that the N1 amplitudes were decreased in *Shank3* mutants compared with WT controls in response to dog and human faces [$F(1,48) = 14.443$ and 5.724, $P < 0.001$ and 0.021; LMM results, $z = -2.597$ and -1.727, $P < 0.01$, $P = 0.084$] but not to houses [$F(1,48) = 2.713$, $P = 0.106$; LMM results, $z = -0.817$, $P = 0.413$]. The N1 amplitudes to dog and human faces did not differ significantly in either WT or *Shank3* mutants ($P > 0.3$). The N1 peak latencies also showed distinct patterns in WT and *Shank3* mutants such that *Shank3* mutants compared to WT showed longer N1 peak latencies to dog and human faces [dog face, $F(1,48) = 16.611$, $P < 0.001$; human face, $F(1,48) = 7.414$, $P = 0.009$] but not to houses [$F(1,48) = 0.339$, $P = 0.563$; Fig. 3D].

ANOVAs of the mean P1 and P2 amplitudes also showed a significant main effect of stimulus category [P1, $F(2,96) = 6.858$, $P = 0.002$; LMM results, $F(2,14,029) = 6.013$, $P = 0.002$; P2, $F(2,96) = 15.666$, $P < 0.001$; LMM results, $F(2,14,029) = 33.131$, $P < 0.001$; Fig. 3, E to H]. However, there were no consistent statistical results that show that the effect of stimulus category differed significantly between WT and *Shank3* mutants [P1, $F(2,96) = 0.84$, $P = 0.435$; LMM results, $F(2,14,029) = 1.107$, $P = 0.331$; P2, $F(2,96) = 1.93$, $P = 0.151$; LMM results, $F(2,14,029) = 4.374$, $P = 0.013$]. There was a significant main effect of stimulus category on the P2 (but not P1) peak latencies [P1, $F(2,96) = 2.088$, $P = 0.13$; P2, $F(2,96) = 6.910$, $P = 0.002$]. Similarly, there was no evidence that the effect of stimulus category on the P1 and P2 peak latencies differed significantly between WT and *Shank3* mutants ($P > 0.5$).

Together, the convergent statistical results indicate that the face-specific neural process in the N1 time window was decreased and delayed in *Shank3* mutants compared to WT dogs. Although the P1 and P2 amplitudes seemed to be sensitive to face stimuli, there was no reliable evidence that these face-sensitive effects were influenced by *Shank3* mutation.

Loss of behavioral preferences for faces of own species/breed in *Shank3* mutants

The ability to recognize faces of conspecifics and heterospecifics is critical for animals' survival (*40*). Thus, we further investigated whether the effect of *Shank3* mutation would extend to the ability to recognize faces based on species or breeds. WT controls and *Shank3* mutants were first tested in the approach-avoidance task using paired face photos of different species or breeds (Fig. 4A). Inverted faces were

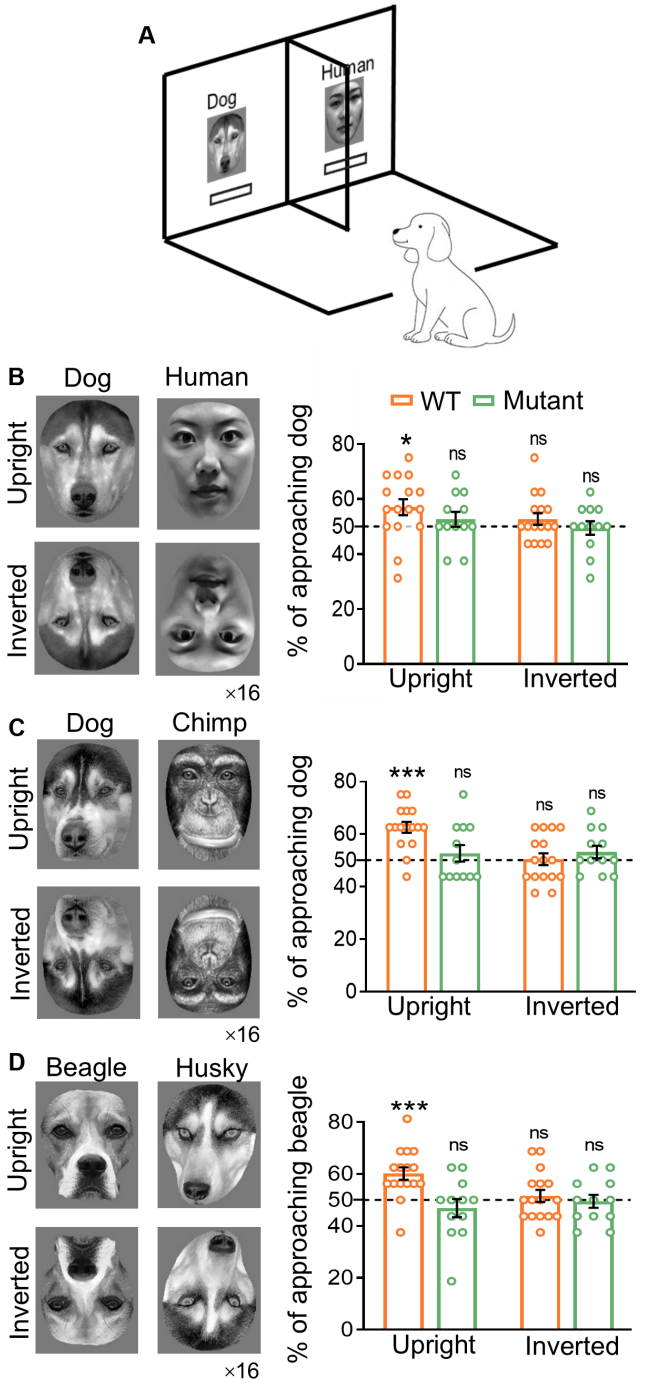

Fig. 4. Loss of behavioral preferences for own species and own breed in *Shank3* mutant dogs. (**A**) Illustration of the behavioral preference–avoidance test. Two faces of different species or breeds were displayed on the monitors simultaneously either in upright or inverted positions. (**B**) Examples of dog/human face stimuli and the results of behavioral preference. There were a total of 16 different pairs in each session. Each photo of 20.3 cm by 25.4 cm was displayed in the center of a 23.7-inch (60.198-cm) monitor. (**C**) Examples of dog/chimpanzee face stimuli and the results of behavioral preference. (**D**) Examples of beagle/husky face stimuli and the results of behavioral preference. WT, $n = 16$; mutants, $n = 12$. Data are presented as means ± SEM. The colored circles represent data points of individual animals. *$P < 0.05$; ***$P < 0.001$; ns, not significant. Human faces from N. Strohminger *et al.* 2016, licensed under Creative Commons Attribution Non-Commercial ShareALike 3.0 Unported License (*63*).

also used in the task to examine whether configural properties are necessary for behavioral preferences as shown in Fig. 1. Because looking preferences are influenced by visual experiences (i.e., familiarity) in infants and nonhuman primates (*41*, *42*), WT dogs might be attracted by conspecific faces. The results showed that WT approached dog (against human) faces more frequently than the chance level of 50% [57.0 ± 2.9%, $t(15) = 2.423$, $P = 0.029$; Fig. 4B], whereas *Shank3* mutants failed to show such a preference [52.6 ± 2.72%, $t(11) = 0.959$, $P = 0.358$]. Similar analyses of behavioral responses to inverted faces failed to show preferences for own species in both WT and *Shank3* mutant dogs ($P > 0.2$). The approach-avoidance task using chimpanzee and dog faces revealed further evidence for own-species preference in WT but not in *Shank3* mutations. WT approached dog (against chimpanzee) faces more frequently than the chance level of 50% [62.5 ± 2.06%, $t(15) = 6.076$, $P < 0.001$; Fig. 4C], but no such preference was found in *Shank3* mutants (52.6 ± 3.12%, $P = 0.422$). Similarly, behavioral responses to inverted faces failed to show preference for dog (against chimpanzee) faces in both WT and *Shank3* mutants ($P > 0.2$). These results suggest that configural properties of faces were necessary for inducing behavioral preferences for conspecific dog faces that were observed in WT controls but not in *Shank3* mutants.

We also examined WT controls and *Shank3* mutants in the approach-avoidance task using dog faces of two different breeds (i.e., beagle and husky; Fig. 4D). WT but not *Shank3* mutants approached beagle (against husky) faces at an above-chance level [WT, 60.2 ± 2.41% versus 50%, $t(15) = 4.21$, $P < 0.001$; mutants, 46.9 ± 3.48% versus 50%, $t(11) = 0.897$, $P = 0.389$]. However, no evidence was found for behavioral preference for inverted beagle faces in either WT or *Shank3* mutants ($P > 0.120$). Together, these results of WT controls revealed behavioral preferences for faces of own species or own breed that depended on configural properties of faces. While these results demonstrated an ability to categorize faces of different species/breeds in WT controls, this ability was lost in *Shank3* mutants.

Loss of attentional bias to faces of own species/breed in *Shank3* mutants

Next, we tested whether *Shank3* mutations also impaired attentional bias to faces of own species by tracking eye movements when WT and *Shank3* mutants viewed two simultaneously displayed photos of a human face and a dog face (Fig. 5, A and B). The results showed that the percentage of gaze duration on dog (against human) faces

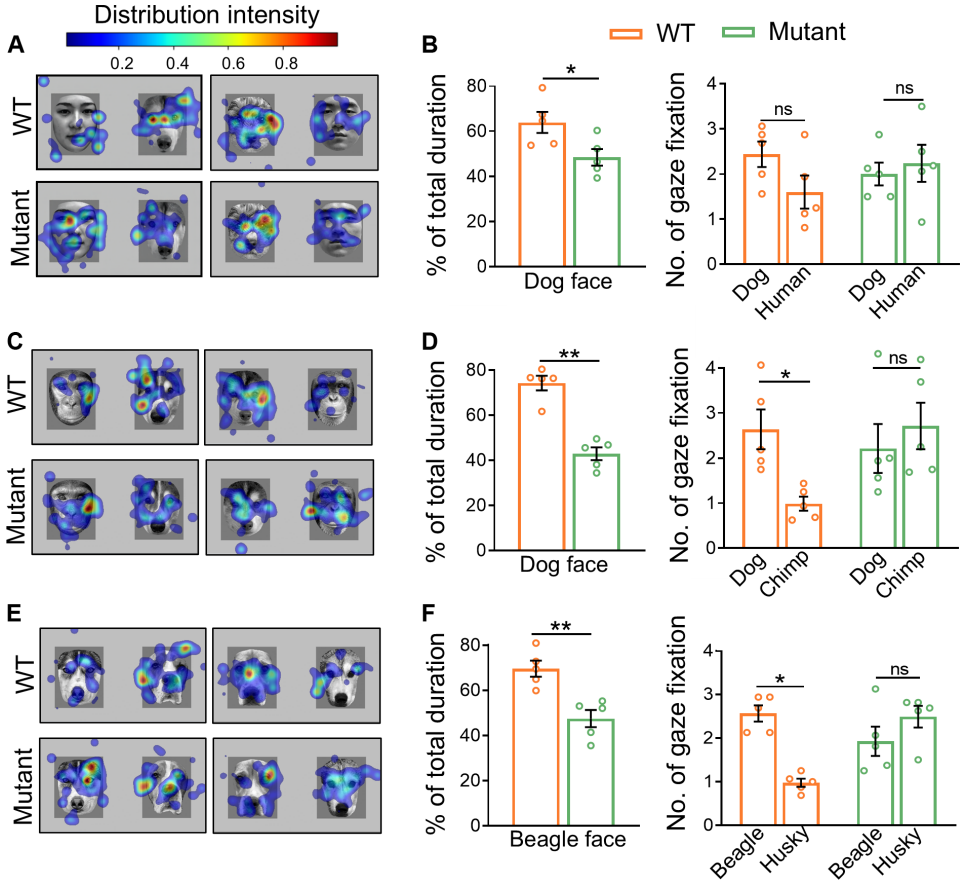

Fig. 5. Loss of eye-gaze preferences for faces of own species/breed in *Shank3* mutant dogs. (**A**) Heatmaps of fixation durations on dog and human faces. (**B**) The mean percentage of fixation durations and the number of gaze fixations on dog and human faces. (**C**) Heatmaps of fixation durations on dog and chimpanzee faces. (**D**) The mean percentage of fixation durations and the mean number of gaze fixations on dog and chimpanzee faces. (**E**) Heatmaps of fixation durations to beagle and husky faces. (**F**) The mean percentage of fixation durations and the number of gaze fixations to beagle and husky faces. WT, $n = 5$; mutants, $n = 5$. Data are presented as means ± SEM. The colored circles represent data points of individual animals. *$P < 0.05$; **$P < 0.01$; ns, not significant. Human faces from N. Strohminger *et al*. 2016, licensed under Creative Commons Attribution Non-Commercial ShareALike 3.0 Unported License (*63*).

was higher than *Shank3* mutants (63.8 ± 4.68% versus 48.4 ± 3.66%, $U = 2$, $P = 0.016$). There was no significant difference between WT and *Shank3* mutants on gaze fixations on dog and human faces ($P > 0.1$). We also replicated the experiment using dog and chimpanzee faces. WT fixated on dog (against chimpanzee) faces longer than *Shank3* mutants (74.2 ± 3.24% versus 42.9 ± 2.84%, $U = 0$, $P = 0.004$; Fig. 5, C and D). We also found that WT but not *Shank3* mutants showed significantly more gaze fixations on dog than on chimpanzee faces (WT, $Z = -2.032$, $P = 0.031$; mutants, $Z = -1.214$, $P = 0.156$).

The patterns of gaze allocations also revealed attentional bias toward faces of own breed in WT controls. WT gazed at beagle (against husky) faces longer than *Shank3* mutants (69.6 ± 3.58% versus 47.4 ± 3.82%, $U = 0$, $P = 0.004$; Fig. 5, E and F). There were significantly more gaze fixations on beagle than on husky faces in WT ($Z = -2.023$, $P = 0.031$) but not in *Shank3* mutants ($Z = -1.214$, $P = 0.156$). These results together demonstrate that the attentional bias toward faces of own species or breed was disrupted in *Shank3* mutants.

Impaired neural categorization of faces in *Shank3* mutants

The above behavioral preferences are based on the ability to categorize faces. We then examined whether *Shank3* mutations affected neural processing involved in the categorization of faces by species and breeds. We recorded and analyzed ECoG signals from WT and *Shank3* mutants in response to face stimuli in a repetition suppression (RS) paradigm developed in studies of social categorization in human faces (*27*). Dog and human faces were presented in the same block of trials in the alternating condition but in separate blocks of trials in the repetition condition (Fig. 6A). Faces with different identities were presented in a random order in both conditions. Decreased ECoG signals to dog (or human) faces in the repetition compared to alternating conditions were quantified to indicate RS effect on neural responses underlying facial categorization, following published protocols (*27*).

We focused on the analyses of potential RS effect in the frontal-parietal region, as this brain region showed robust neural activities specific to face categorization in humans (*27*, *43*, *44*). Face stimuli elicited an early negative activity (N1; 44 to 71 ms), a following positive activity (P1; 86 to 107 ms), and a late negative activity (N2; 203 to 245 ms) at the frontal-parietal electrodes (Fig. 6, B and C, also see fig. S6 for evoked potentials recorded at the temporal electrodes). ANOVAs of the mean P1 amplitudes with *stimulus* (human versus dog faces) and *condition* (repetition versus alternating) as within-subjects factors and *group* (WT versus *Shank3* mutants) as a between-subjects factor revealed a significant three-way interaction [$F(1,48) = 4.740$, $P = 0.034$; LMM results, $F(1,18,763) = 6.663$, $P < 0.01$; Fig. 6D and table S5], indicating distinct patterns of the RS effects in WT and *Shank3* mutants. Separate analyses verified significant RS of the P1 amplitudes to human faces [$F(1,48) = 9.453$, $P = 0.003$; LMM results, $z = 3.501$, $P < 0.001$] but not to dog faces [$F(1,48) = 1.620$, $P = 0.209$; LMM results, $z = -1.512$, $P = 0.131$] in WT, indicating early neural categorization of human faces. However, the P1 amplitudes failed to show RS to human or dog faces in *Shank3* mutants ($P > 0.5$). A significant three-way interaction was also evident on the N2 amplitude [$F(1,48) = 5.583$, $P = 0.022$; LMM results, $F(1,18,763) = 6.014$, $P = 0.014$; Fig. 6E]. Separate analyses revealed RS of the N2 amplitudes to dog faces [$F(1,48) = 25.988$, $P < 0.001$; LMM results, $z = -4.847$, $P < 0.001$] but not to human faces [$F(1,48) = 0.162$, $P = 0.689$; LMM results, $z = 0.240$, $P = 0.810$] in WT, suggesting late neural categorization of dog faces. Again, no RS of the N2 amplitudes to faces was found in *Shank3* mutants ($P > 0.8$; Fig. 6E). Similar analyses of the cortical responses of N1 (83 to 107 ms) and P2 (206 to 252 ms) amplitudes at the temporal electrodes only showed a significant RS effect of the P2 amplitude to dog faces in WT [$F(1,48) =$, $P < 0.001$; LMM results, $z = 3.989$, $P < 0.001$; fig. S6].

The same design was used to record ECoG signals to beagle (own breed) and husky (other breed) faces from WT and *Shank3* mutant dogs. ANOVAs of the mean P1 amplitudes showed a significant three-way interaction [$F(1,48) = 6.728$, $P = 0.013$; LMM results, $F(1,18,842) = 9.929$, $P = 0.002$; also see table S6]. Separate analyses revealed RS of the P1 amplitudes to husky faces [$F(1,48) = 49.638$, $P < 0.001$; LMM results, $z = 7.085$, $P < 0.001$; Fig. 6H] but not to beagle faces [$F(1,48) = 0.029$, $P = 0.867$; LMM results, $z = -0.198$, $P = 0.843$] in WT, suggesting RS of early neural responses to other-breed faces. However, no RS effect was observed for the P1 amplitudes in *Shank3* mutants ($P > 0.3$). ANOVAs of the mean N2 amplitudes showed neither a significant RS effect in both WT and *Shank3* mutants ($P > 0.7$) nor a significant three-way interaction effect ($P > 0.2$; table S6). Similar analyses of the cortical responses at the temporal electrodes also showed a significant interaction effect on the N1 (86 to 112 ms) amplitudes [$F(1,48) = 6.438$, $P = 0.014$; LMM results, $F(1,18,762) = 7.524$, $P = 0.006$; fig. S6]. Simple effect analyses further revealed RS of the N1 amplitudes to husky faces [$F(1,48) = 63.14$, $P < 0.001$; LMM results, $z = -7.607$, $P < 0.001$] but not to beagle faces in WT. However, no RS effect was observed for the N1 amplitudes in *Shank3* mutants ($P > 0.3$; fig. S6).

Together, the statistical analyses of the ECoG signals showed convergent evidence for two successive neural processes that supported categorization of other-species/breed and own-species faces, respectively, in WT controls. *Shank3* mutants, however, showed impaired neural processes involved in face categorization by species or breeds.

DISCUSSION

Building genetic models with behavioral and cognitive deficits similar to those in human patients is critical for dissecting the pathophysiological mechanisms of human brain disorders and for developing effective interventions (*45*). Built on *Shank3* mutant dogs (*19*), the current work established a dog model of ASD-like atypical face processing that is difficult or even impossible to simulate in rodents and nonhuman primates. Furthermore, our work demonstrates that mutations in an autism risk gene, i.e., *Shank3*, lead to ASD-like atypical face processing.

Our results demonstrate ASD-like face processing deficits at two levels in the dog model with *Shank3* mutations. First, WT dogs showed behavioral preferences and attentional biases to faces over nonface stimuli (i.e., houses), similar to the findings in humans (*46*, *47*) and nonhuman primates (*42*). *Shank3* mutant dogs, however, exhibited ASD-like behavioral and eye-gaze avoidance of faces (particularly the eye regions), paralleling the findings of reduced face attention (*48*) and preference for nonsocial stimuli (*49*) in children with ASD. Moreover, WT dogs showed a face-specific neural response, i.e., the N1 response, at the electrodes over the temporal cortex around 100 ms poststimulus. The N1 response in dogs occurred earlier than the face-sensitive N170 response that peaked at

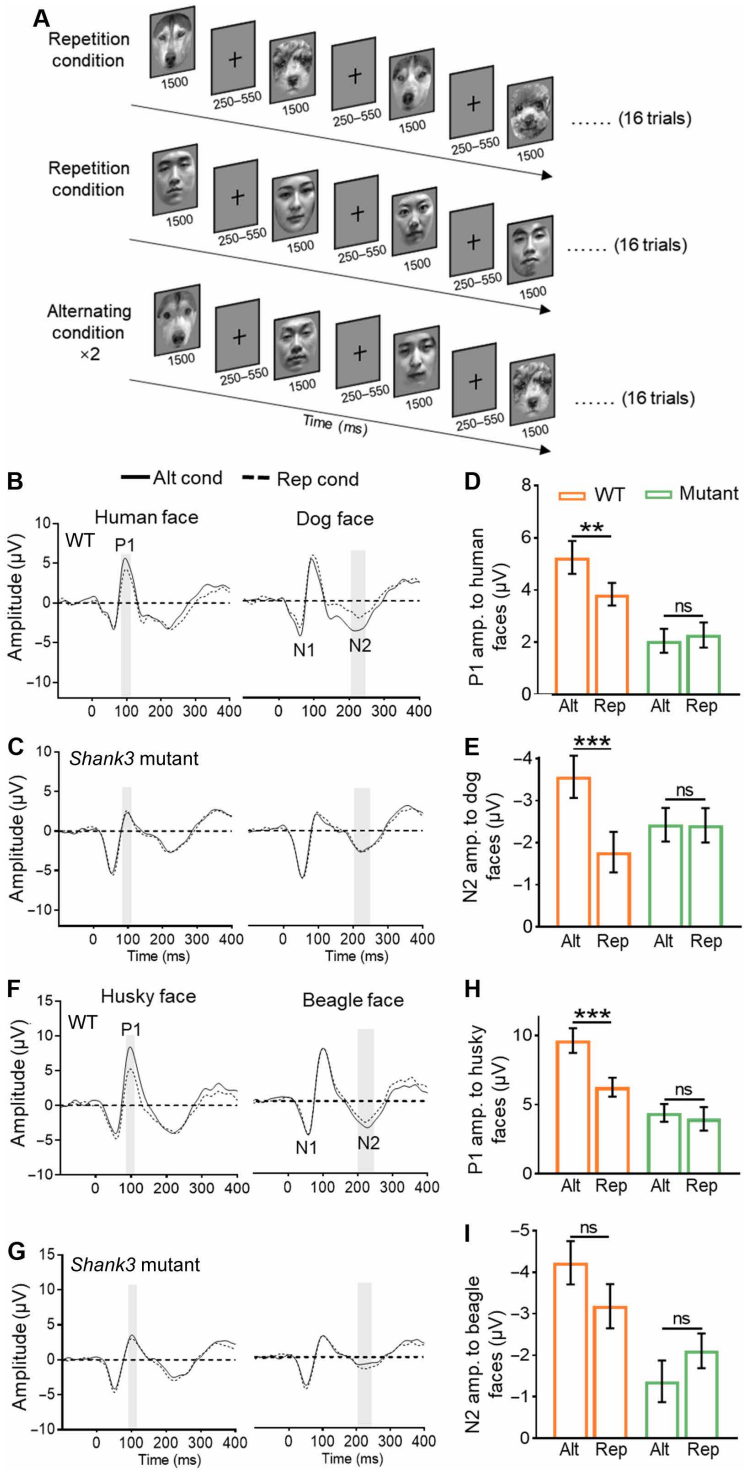

Fig. 6. Impaired neural responses related to facial categorization in *Shank3* mutant dogs. (**A**) Illustrations of the stimuli and procedures of the RS paradigm. Each run consisted of four blocks of 16 trials [including two repetition (Rep) blocks and two alternating (Alt) blocks]. (**B** and **C**) ERPs to human and dog faces at the frontal/parietal electrodes in the alternating and repetition conditions (cond) in WT ($n = 5$) and mutant dog ($n = 5$). (**D** and **E**) The mean P1 and N2 amplitudes (amp.) in response to human and dog faces in each condition. (**F** and **G**) ERPs to beagle and husky faces at the frontal/parietal electrodes in the alternating and repetition conditions in WT ($n = 5$) and mutant dog ($n = 5$). (**H** and **I**) The mean P1 and N2 amplitudes in response to husky faces and beagle faces in each condition. Significance of the ANOVA results was noted in the figure. Data are presented as means ± SEM. The gray bar indicates the time window used for analysis. $^{**}P < 0.01$; $^{***}P < 0.001$; ns, not significant. Human faces from N. Strohminger *et al*. 2016, licensed under Creative Commons Attribution Non-Commercial ShareALike 3.0 Unported License (*63*).

170 ms after stimulus onset observed in scalp ERPs in humans (*50*) with sources in the fusiform and occipital face areas (*51*). The latency of the face-specific N1 activity in WT dogs was, however, similar to that of the face-specific monkey N1 (mN1) response identified in monkeys (*52*) that may also originate from the ventral temporal cortex as suggested by the studies using single-unit recording (*53*). These findings indicate early face perception as a common ability crucial for social interactions across species and suggest possible species-specific adaptations in how fast the early neural coding of faces takes place. We found evidence that *Shank3* mutants compared to WT controls showed decreased and delayed N1 responses specific to faces in the temporal region, akin to the finding of decreased and delayed neurophysiological responses to faces in patients with ASD compared to healthy controls (*54*).

Second, WT dogs showed consistent evidence for spontaneous categorization of faces of other (versus own) species or breed in behavioral preferences, attentional biases, and neural responses to faces. Specifically, they showed a delayed neural categorization of faces of own species but early neural categorization of faces of other species. This ability may help animals to detect other unfamiliar species, enabling them to better survive. While *Shank3* mutants failed to display any sign of processing high-level facial information that supported the social categorization of faces by species and breeds, the lack of preferences for faces of own species or breed in *Shank3* mutant dogs cannot be simply attributed to ignorance of the visual stimuli because *Shank3* mutants' eye gaze did fall on the face stimuli. The combination of behavioral, eye-tracking, and ECoG results together demonstrates that *Shank3* mutations in dogs disrupt the two levels of face processing. We suspect that the lack of innate, first-level face (versus house) preference may explain the impairment of experience-dependent, second-level face categorization in *Shank3* mutants. Note that the neural response to face (versus house) is evidently detected in the temporal cortex, while the face categorization occurs largely in the frontal/parietal cortices of dogs.

Our findings highlight a previously unappreciated role for *Shank3* in face processing. Studies of human twins revealed that performances in face recognition (*9*, *10*), face preference (*11*), and the neural response to faces (*55*) showed greater correlations in monozygotic twins than in dizygotic twins. These results, consistent with the findings of selectively impaired visual learning and recognition of faces in family members (*56*, *57*), indicate that the ability to memorize and recognize faces and the underlying face-specific neural processes are heritable. Our work provided valuable experimental evidences that mutations of an ASD-associated gene caused impaired perceptual discrimination of faces versus nonface objects and categorization of faces based on species and breeds. In addition, our electrophysiological findings revealed the underlying neural activities of impaired face processing, i.e., decreased and delayed temporal N1 response specific to faces (versus objects) and the decreased frontal/parietal P1/N2 responses specific to categorization of faces. While the etiology for the atypical face processing in ASD remains uncharacterized, the finding of impaired face processing in *Shank3* mutant dogs offers an insight into the genetic basis of the atypical face processing in ASD.

The findings of the current work demonstrate *Shank3* mutant dogs as a valid animal model for further mechanistic investigation of impaired face processing in ASD. First, patients with ASD exhibit impaired gender and emotion categorization of faces (*58*, *59*) and deficits in face recognition that engage perception and memory of identities of individual faces (*2*). Given the dogs' abilities to differentiate identities and emotions of both dog and human faces (*60*), it would be interesting to test whether *Shank3* mutations in dogs also cause ASD-like deficits in recognition of facial identity and expression. Second, our ECoG results provide temporal information about the two levels of face processing [i.e., early discrimination of face versus nonface object (N1, 89 to 123 ms) and subsequent categorization of own-species (N2, 203 to 245 ms) versus other-species/breed faces (P1, 86 to 107 ms)] that were affected by *Shank3* mutations in dogs. Future research may integrate the dog model presented here with other methods such as those used in monkey studies of face processing (*61*, *62*) to examine the neural networks and cell types that are involved in face processing and affected by *Shank3* mutations. Last, but not least, *SHANK3* is one of the hundreds of high-risk genes for ASD (https://sfari.org/resource/sfari-gene/) (*6*). Future research should clarify whether mutations in other ASD high-risk genes would also lead to ASD-like atypical face processing or other cognitive deficits in dog models.

MATERIALS AND METHODS

Subjects

A total of 23 WT (beagles) from Sinogene Ltd. (Beijing, China) and 15 *Shank3* mutant dogs (beagles) were tested in this study. The mean age did not differ significantly between WT controls and *Shank3* mutants [WT, 19.3 ± 1.33 months of age (mean ± SEM); mutants, 24.5 ± 2.75 months of age, $U = 125.5$, $P = 0.164$; see tables S1 and S2 for detailed information about the subjects in each experiment]. Four WT controls (80, 201138, 210755, and 201115) and three *Shank3* mutants (201111, 201112, and 201141) were tested in a previous behavioral study of dog-human interactions (*19*). Two *Shank3* mutants (190203 and 190604) were tested in an ECoG study that required the subjects to passively listen to pure sinusoidal tones (*26*). None of these studies involved any training with food or used stimuli of animal/human faces or houses. Three dogs tested in this work were littermates [i.e., WT (201115) and *Shank3* mutants (201111 and 201112)]. WT (201115) participated in experiment 1. *Shank3* mutant 201111 participated in experiments 1 and 4. *Shank3* mutant 201112 participated in experiment 4. The *Shank3* mutations generate frameshifts and truncated proteins, disrupting the ankyrin (ANK) domain and proline-rich domain of *Shank3* in mutant dogs (*19*). All mutant dogs showed a similarly reduced level of *Shank3* protein and similar autism-like social deficits, including social withdrawal and reduced social interactions with humans (*19*). Each dog was housed in a single cage and maintained on a 12-hour light/12-hour dark cycle with lights on at 7:00 a.m. All subjects were submitted to ophthalmological and behavioral evaluation to verify their healthy conditions before the study. No animal was euthanized in these studies. All experimental procedures were approved by the Ethical Committee of the Institute of Genetics and Developmental Biology of the Chinese Academy of Sciences (AP2022033).

Visual stimuli

The visual stimuli used in the present study included photos of 16 human faces, 16 beagle faces, 24 husky faces, 8 poodle faces, 16 chimpanzee faces, 16 cars, and 16 houses. Black-and-white stimuli were used to control potential effects of color differences between face and house stimuli. The details of the stimuli used for each experiment are shown in tables S1 and S2. The human faces were adopted from previous work (*63*). Chimpanzee, dog faces, and cars were collected from public internet image resources. Faces of full-frontal views with eyes open,

direct forward gaze, and neutral expression were used. All the images were unfamiliar to the subjects. Luminance and contrast were matched for images of each category using the SHINE toolbox in MATLAB and for images of different categories. All images were presented on a gray background (122 cd/m^2). The stimuli produced a 20.3 cm–by–25.4 cm picture (resolution, 800 pixels by 1000 pixels) on the center of the screens, positioned 240 cm away from the subject in face preference tests. In the electrophysiological experiments, each stimulus with a resolution of 400 pixels by 500 pixels was displayed on a 23.7-inch (60.198-cm) screen, positioned approximately 65 cm to the subject.

Behavioral preference test

The experimental setup was modified from an approach-avoidance test in a previous study (*33*), as illustrated in Fig. 1A. The setup included a food tray placed close to the bottom of a computer monitor on each side of the room. The two sets of food trays and monitors were separated by a board. Before the experiment, a dog was allowed to move freely in the test room for about 10 min. Thereafter, the experimenter turned the dog around with its back facing the two monitors. At the beginning of each trial, two identical dog snacks were placed on each of the trays. A pair of photos of two different categories was then randomly displayed on the left and right monitors (Fig. 1B). The photos of the two stimuli used in each trial varied randomly across trials. The test dog was guided to sit in the middle of the testing room facing the monitors for 3 to 5 s before being released to walk toward a food tray. After eating the snack on one food tray, the subject was led back to the release point for the next trial. A subject was tested in 16 trials for 15 to 45 min/day. If a test dog did not approach one of the two sides with different photo stimuli in a trial, then the test was terminated.

Eye movement recording

The preferential viewing task was adapted from a previous study (*64*) for the eye-tracking measurements after the calibration procedure using the EyeLink five-point calibration program. The experimenter guided the dogs through finger tapping or food cues to ensure their gaze fixation on the calibration point. The experimenter then repeated the five-point calibration again to get the value of calibration accuracy. Subjects seated or stood approximately 85 cm away from a 23.7-inch (60.198-cm) liquid crystal display monitor (resolution, 1920 pixels by 1080 pixels) when viewing the stimuli. Eye movements were recorded at a sampling rate of 500 Hz using an EyeLink 1000 Plus eye tracker (SR Research Ltd., Mississauga, Ontario, Canada). Each trial started with a moving circle that caught a subject's attention toward the center of the monitor. Once a fixation on the circle lasted longer than 100 ms, two stimuli of different categories were presented simultaneously on the left and the right sides of the screen in a random order across trials for 3 s, similar to the paradigm used in previous studies of humans (*65*). Eye-tracking data during the presentation of the stimuli were analyzed. Eye-tracking measurements were conducted in experiment 2 using photos of dog faces and houses and in experiment 4 using photos of dog/human faces, dog/chimpanzee faces, and beagle/husky faces. In each experiment, a subject was tested in 16 trials using each set of face stimuli. Additional trials were performed in case of failed trials to ensure the completion of 16 trials for each experiment.

ECoG data recording

ECoG signals were recorded from 32 electrodes over the right hemisphere that covered the frontal, parietal, temporal, and occipital cortices using the protocol described in previous research (fig. S2) (*26*). Each electrode disc was 2.0 mm in diameter and spaced 5 mm apart. Electrode positions were verified using computer tomography scans. ECoG recordings were performed in a sound-attenuated room with dim light. Zeus data acquisition system (Zeus, Nanjing, China) was used to record ECoG signals with a sampling rate of 1 kHz. The subject was seated approximately 65 cm from the computer screen that was positioned to ensure that the stimulus was placed at the center of the screen. During ECoG recording, a dog was instructed to sit on the ground or on the experimenter's lap. A camera was set to allow the experimenter to monitor the subject's gaze. Each trial in experiment 3 started with the presentation of an image of a face or houses for 1500 ms in the center of the gray background. This was followed by a fixation cross with a duration varying randomly from 250 to 550 ms. Each subject was tested in four to six sessions on separate days, and there were six runs in each session. Each run consisted of two blocks of 24 trials. There was a 5-s break between two consecutive blocks. In experiments 6 and 7, ECoG was recorded in an RS paradigm in five sessions. There were six runs in each session and there were four blocks of 16 trials in each run. The stimulus duration and interstimulus interval were the same as those in experiment 3.

Behavioral data analysis

We quantified behavioral preferences for faces (against houses) as the percentage of trials in which a dog walked toward a face photo and preferences for houses (against cars) as the percentage of trials in which a dog initially walked toward a house photo in experiment 1. Behavioral preferences in experiment 4 were quantified as the percentage of trials in which a dog walked toward faces of own species (against human or chimpanzee faces) or breed (against husky faces). One-sample *t* tests were conducted to assess behavioral preferences for faces (or faces of a specific species) in experiments 1 and 4.

Eye-tracking data analysis

We first quantified the ratio of time devoted to observing various categories of stimuli in relation to the total looking time in each trial. Trials with less than 25% screening-looking time were considered invalid and excluded from data analyses. We defined the area on the left side of the screen, which encompasses the width subtracted from the fixation point to the center, as area of interest 1 (AOI-1) and the area on the right side of the screen, which encompasses the width subtracted from the fixation point to the center, as AOI-2. The two AOIs independently represent the two different pictures in each trial. The AOIs were determined for faces and house stimuli in experiment 2 and for faces of different species/breeds in experiment 5. We also defined the area of eye region in experiment 2 as AOI-3. By calculating the duration of all fixations falling inside each AOI in each trial, we obtained the total looking time on the target region for each trial. Because eye-tracking data do not follow a normal distribution, we used the nonparametric Mann-Whitney test to access statistical differences in behaviors between the two testing groups (i.e., WT controls and *Shank3* mutants) and the nonparametric Wilcoxon signed-rank test to assess differences in behaviors between two measures in one testing group (e.g., gaze fixations on faces versus house in WT controls). These statistical methods were applied similarly to individual-based data analyses (see results in experiments 2 and 5) and trial-based data analysis (see results in the Supplementary Materials and figs. S1 and S5). Heatmap of the gaze distribution was drawn through a Python

toolbox GazePointHeatMap (https://github.com/TobiasRoeddiger/GazePointHeatMap) based on the viewing time of the stimuli.

ECoG data analysis

ECoG data analyses were performed using MATLAB (version 2020b, MathWorks Inc., Natick, MA) and the EEGLAB toolbox. During preprocessing, the ECoG signals were rereferenced using a common average reference montage and band-pass filtered from 0.1 to 30 Hz. ERPs in each condition were averaged separately offline with an epoch beginning 200 ms before stimulus onset and continuing for 600 ms after stimulus onset. Trials contaminated by noises exceeding ±200 μV at any electrode were excluded from the average analysis. The baseline for ERP measurements was the mean voltage across a 200-ms prestimulus time window. The latency was measured relative to the stimulus onset.

The time windows of peak responses were independently defined for each ERP component in each experiment (see table S3 for details). The mean amplitudes and peak latencies of the P1, N1, and P2 components in experiment 3 were subjected to repeated-measures ANOVAs with stimulus category (human face versus dog face versus house) as a within-subjects factor and testing group (WT versus *Shank3* mutants) as a between-subjects factor. The mean P1 and N2 amplitudes in experiments 6 and 7 were subject to ANOVAs with stimulus categories (human versus dog faces or beagle versus husky) and conditions (repetition versus alternating conditions) as within-subjects factors and group (WT versus mutants) as a between-subjects factor. RS effects were defined as decreased amplitudes to faces of a category in the repetition compared to alternating conditions.

To further verify the ERP results shown in ANOVAs by controlling potential effects of within-subject correlations, we conducted LMM analyses of the ERP data. The statistical analyses of single-trial ECoG amplitudes were conducted using mixed-effect single-trial regression models, similar to the method of a previous work (*66*). The fixed-effect factors included stimuli (first level, −0.67 for house, +0.33 for human, and +0.33 for dog; second level, −0.33 for house, −0.33 for human, and +0.67 for dog), testing group (−0.5 for WTs and +0.5 for *Shank3* mutants), and their interactions in experiment 3. In experiments 6 and 7, the fixed-effect factors included stimuli (−0.5 for dog/beagle faces and +0.5 for human/husky faces), condition (−0.5 for the alternating condition and +0.5 for the repetition condition), testing group (−0.5 for WTs and +0.5 for *Shank3* mutants), and their interactions. Subjects' identities (ID) and the recording sessions of each subject were included as the nested random-effect factors.

Supplementary Materials

This PDF file includes:

Supplementary Text
Figs. S1 to S6
Tables S1 to S6

REFERENCES AND NOTES

1. American Psychiatric Association, *Diagnostic and Statistical Manual of Mental Disorders* (American Psychiatric Press, ed. 5, 2013).
2. J. W. Griffin, R. Bauer, K. S. Scherf, A quantitative meta-analysis of face recognition deficits in autism: 40 years of research. *Psychol. Bull.* **147**, 268–292 (2021).
3. J. Osterling, G. Dawson, Early recognition of children with autism: A study of first birthday home videotapes. *J. Autism Dev. Disord.* **24**, 247–257 (1994).
4. I. A. J. van Kooten, S. J. M. C. Palmen, P. von Cappeln, H. W. M. Steinbusch, H. Korr, H. Heinsen, P. R. Hof, H. van Engeland, C. Schmitz, Neurons in the fusiform gyrus are fewer and smaller in autism. *Brain* **131**, 987–999 (2008).
5. K. Pierce, R. A. Müller, J. Ambrose, G. Allen, E. Courchesne, Face processing occurs outside the fusiform 'face area' in autism: Evidence from functional MRI. *Brain* **124**, 2059–2073 (2001).
6. B. S. Abrahams, D. E. Arking, D. B. Campbell, H. C. Mefford, E. M. Morrow, L. A. Weiss, I. Menashe, T. Wadkins, S. Banerjee-Basu, A. Packer, SFARI Gene 2.0: A community-driven knowledgebase for the autism spectrum disorders (ASDs). *Mol. Autism.* **4**, 36 (2013).
7. B. S. Abrahams, D. H. Geschwind, Advances in autism genetics: On the threshold of a new neurobiology. *Nat. Rev. Genet.* **9**, 341–355 (2008).
8. B. Yuan, M. Wang, X. Wu, P. Cheng, R. Zhang, R. Zhang, S. Yu, J. Zhang, Y. Du, X. Wang, Z. Qiu, Identification of de novo mutations in the Chinese autism spectrum disorder cohort via whole-exome sequencing unveils brain regions implicated in autism. *Neurosci. Bull.* **39**, 1469–1480 (2023).
9. Q. Zhu, Y. Song, S. Hu, X. Li, M. Tian, Z. Zhen, Q. Dong, N. Kanwisher, J. Liu, Heritability of the specific cognitive ability of face perception. *Curr. Biol.* **20**, 137–142 (2010).
10. N. G. Shakeshaft, R. Plomin, Genetic specificity of face recognition. *Proc. Natl. Acad. Sci. U.S.A.* **112**, 12887–12892 (2015).
11. A. M. Portugal, C. Viktorsson, M. J. Taylor, L. Mason, K. Tammimies, A. Ronald, T. Falck-Ytter, Infants' looking preferences for social versus non-social objects reflect genetic variation. *Nat. Hum. Behav.* **8**, 115–124 (2024).
12. R. Moessner, C. R. Marshall, J. S. Sutcliffe, J. Skaug, D. Pinto, J. Vincent, L. Zwaigenbaum, B. Fernandez, W. Roberts, P. Szatmari, S. W. Scherer, Contribution of *SHANK3* mutations to autism spectrum disorder. *Am. J. Hum. Genet.* **81**, 1289–1297 (2007).
13. X. Wang, A. L. Bey, B. M. Katz, A. Badea, N. Kim, L. K. David, L. J. Duffney, S. Kumar, S. D. Mague, S. W. Hulbert, N. Dutta, V. Hayrapetyan, C. Yu, E. Gaidis, S. Zhao, J. D. Ding, Q. Xu, L. Chung, R. M. Rodriguiz, F. Wang, R. J. Weinberg, W. C. Wetsel, K. Dzirasa, H. Yin, Y.-H. Jiang, Altered mGluR5-Homer scaffolds and corticostriatal connectivity in a *Shank3* complete knockout model of autism. *Nat. Commun.* **7**, 11459 (2016).
14. J. Peça, C. Feliciano, J. T. Ting, W. Wang, M. F. Wells, T. N. Venkatraman, C. D. Lascola, Z. Fu, G. Feng, *Shank3* mutant mice display autistic-like behaviours and striatal dysfunction. *Nature* **472**, 437–442 (2011).
15. A. L. Bey, X. Wang, H. Yan, N. Kim, R. L. Passman, Y. Yang, X. Cao, A. J. Towers, S. W. Hulbert, L. J. Duffney, E. Gaidis, R. M. Rodriguiz, W. C. Wetsel, H. H. Yin, Y.-h. Jiang, Brain region-specific disruption of *Shank3* in mice reveals a dissociation for cortical and striatal circuits in autism-related behaviors. *Transl. Psychiatry* **8**, 94 (2018).
16. Z. Tu, H. Zhao, B. Li, S. Yan, L. Wang, Y. Tang, Z. Li, D. Bai, C. Li, Y. Lin, Y. Li, J. Liu, H. Xu, X. Guo, Y.-H. Jiang, Y. Q. Zhang, X.-J. Li, CRISPR/Cas9-mediated disruption of *SHANK3* in monkey leads to drug-treatable autism-like symptoms. *Hum. Mol. Genet.* **28**, 561–571 (2019).
17. Y. Zhou, J. Sharma, Q. Ke, R. Landman, J. Yuan, H. Chen, D. S. Hayden, J. W. Fisher III, M. Jiang, W. Menegas, T. Aida, T. Yan, Y. Zou, D. Xu, S. Parmar, J. B. Hyman, A. Fanucci-Kiss, O. Meisner, D. Wang, Y. Huang, Y. Li, Y. Bai, W. Ji, X. Lai, W. Li, L. Huang, Z. Lu, L. Wang, S. A. Anteraper, M. Sur, H. Zhou, A. P. Xiang, R. Desimone, G. Feng, S. Yang, Atypical behaviour and connectivity in *SHANK3*-mutant macaques. *Nature* **570**, 326–331 (2019).
18. A. Renard, E. R. Harrell, B. Bathellier, Olfactory modulation of barrel cortex activity during active whisking and passive whisker stimulation. *Nat. Commun.* **13**, 3830 (2022).
19. R. Tian, Y. Li, H. Zhao, W. Lyu, J. Zhao, X. Wang, H. Lu, H. Xu, W. Ren, Q.-Q. Tan, Q. Shi, G.-D. Wang, Y.-P. Zhang, L. Lai, J. Mi, Y.-H. Jiang, Y. Q. Zhang, Modeling *SHANK3*-associated autism spectrum disorder in beagle dogs via CRISPR/Cas9 gene editing. *Mol. Psychiatry* **28**, 3739–3750 (2023).
20. L. Huber, A. Racca, B. Scaf, Z. Viranyi, F. Range, Discrimination of familiar human faces in dogs (*Canis familiaris*). *Learn. Motiv.* **44**, 258–269 (2013).
21. M. Nagasawa, K. Murai, K. Mogi, T. Kikusui, Dogs can discriminate human smiling faces from blank expressions. *Anim. Cogn.* **14**, 525–533 (2011).
22. B. Hare, M. Tomasello, Human-like social skills in dogs? *Trends Cogn. Sci.* **9**, 439–444 (2005).
23. B. Hare, M. Brown, C. Williamson, M. Tomasello, The domestication of social cognition in dogs. *Science* **298**, 1634–1636 (2002).
24. A. M. Thompkins, B. Ramaiahgari, S. Zhao, S. S. R. Gotoor, P. Waggoner, T. S. Denney, G. Deshpande, J. S. Katz, Separate brain areas for processing human and dog faces as revealed by awake fMRI in dogs (*Canis familiaris*). *Learn. Behav.* **46**, 561–573 (2018).
25. N. Bunford, R. Hernández-Pérez, E. B. Farkas, L. V. Cuaya, D. Szabó, A. G. Szabó, M. Gácsi, A. Miklósi, A. Andics, Comparative brain imaging reveals analogous and divergent patterns of species and face sensitivity in humans and dogs. *J. Neurosci.* **40**, 8396–8408 (2020).
26. L. Wu, S. Mei, S. Yu, S. Han, Y. Q. Zhang, Shank3 mutations enhance early neural responses to deviant tones in dogs. *Cereb. Cortex* **33**, 10546–10557 (2023).
27. Y. Zhou, T. Gao, T. Zhang, W. Li, T. Wu, X. Han, S. Han, Neural dynamics of racial categorization predicts racial bias in face recognition and altruism. *Nat. Hum. Behav.* **4**, 69–87 (2020).
28. K. Pierce, S. Marinero, R. Hazin, B. McKenna, C. C. Barnes, A. Malige, Eye tracking reveals abnormal visual preference for geometric images as an early biomarker of an autism spectrum disorder subtype associated with increased symptom severity. *Biol. Psychiatry* **79**, 657–666 (2016).

29. J. McPartland, G. Dawson, S. J. Webb, H. Panagiotides, L. J. Carver, Event-related brain potentials reveal anomalies in temporal processing of faces in autism spectrum disorder. *J. Child Psychol. Psychiatry* **45**, 1235–1245 (2004).
30. E. Di Giorgio, J. L. Loveland, U. Mayer, O. Rosa-Salva, E. Versace, G. Vallortigara, Filial responses as predisposed and learned preferences: Early attachment in chicks and babies. *Behav. Brain Res.* **325**, 90–104 (2017).
31. V. M. Reid, K. Dunn, R. J. Young, J. Amu, T. Donovan, N. Reissland, The human fetus preferentially engages with face-like visual stimuli. *Curr. Biol.* **27**, 1825–1828.e3 (2017).
32. S. Somppi, H. Törnqvist, L. Hänninen, C. Krause, O. Vainio, Dogs do look at images: Eye tracking in canine cognition research. *Anim. Cogn.* **15**, 163–174 (2012).
33. C. M. C. Raoult, L. Gygax, Valence and intensity of video stimuli of dogs and conspecifics in sheep: Approach-avoidance, operant response, and attention. *Animals (Basel)* **8**, 121 (2018).
34. J. S. Husk, P. J. Bennett, A. B. Sekuler, Inverting houses and textures: Investigating the characteristics of learned inversion effects. *Vision Res.* **47**, 3350–3359 (2007).
35. C. J. Mondloch, R. Le Grand, D. Maurer, Configural face processing develops more slowly than featural face processing. *Perception* **31**, 553–566 (2002).
36. K. Chawarska, S. Macari, F. Shic, Decreased spontaneous attention to social scenes in 6-month-old infants later diagnosed with autism spectrum disorders. *Biol. Psychiatry* **74**, 195–203 (2013).
37. A. Klin, W. Jones, R. Schultz, F. Volkmar, D. Cohen, Visual fixation patterns during viewing of naturalistic social situations as predictors of social competence in individuals with autism. *Arch. Gen. Psychiatry* **59**, 809–816 (2002).
38. W. Jones, K. Carr, A. Klin, Absence of preferential looking to the eyes of approaching adults predicts level of social disability in 2-year-old toddlers with autism spectrum disorder. *Arch. Gen. Psychiatry* **65**, 946–954 (2008).
39. N. Kanwisher, J. McDermott, M. M. Chun, The fusiform face area: A module in human extrastriate cortex specialized for face perception. *J. Neurosci.* **17**, 4302–4311 (1997).
40. D. A. Leopold, G. Rhodes, A comparative view of face perception. *J. Comp. Psychol.* **124**, 233–251 (2010).
41. E. Di Giorgio, D. Méary, O. Pascalis, F. Simion, The face perception system becomes species-specific at 3 months: An eye-tracking study. *Int. J. Behav. Dev.* **37**, 95–99 (2013).
42. Y. Sugita, Face perception in monkeys reared with no exposure to faces. *Proc. Natl. Acad. Sci. U.S.A.* **105**, 394–398 (2008).
43. W. A. Cunningham, M. K. Johnson, C. L. Raye, J. C. Gatenby, J. C. Gore, M. R. Banaji, Separable neural components in the processing of black and white faces. *Psychol. Sci.* **15**, 806–813 (2004).
44. T. A. Ito, G. R. Urland, Race and gender on the brain: Electrocortical measures of attention to the race and gender of multiply categorizable individuals. *J. Pers. Soc. Psychol.* **85**, 616–626 (2003).
45. C. G. Jennings, R. Landman, Y. Zhou, J. Sharma, J. Hyman, J. A. Movshon, Z. Qiu, A. C. Roberts, A. W. Roe, X. Wang, H. Zhou, L. Wang, F. Zhang, R. Desimone, G. Feng, Opportunities and challenges in modeling human brain disorders in transgenic primates. *Nat. Neurosci.* **19**, 1123–1130 (2016).
46. M. Buiatti, E. Di Giorgio, M. Piazza, C. Polloni, G. Menna, F. Taddei, E. Baldo, G. Vallortigara, Cortical route for facelike pattern processing in human newborns. *Proc. Natl. Acad. Sci. U.S.A.* **116**, 4625–4630 (2019).
47. C. C. Goren, M. Sarty, P. Y. Wu, Visual following and pattern discrimination of face-like stimuli by newborn infants. *Pediatrics* **56**, 544–549 (1975).
48. J. Vacas, A. Antolí, A. Sánchez-Raya, C. Pérez-Dueñas, F. Cuadrado, Visual preference for social vs. non-social images in young children with autism spectrum disorders. An eye tracking study. *PLOS ONE* **16**, e0252795 (2021).
49. C. M. Gale, S. Eikeseth, L. Klintwall, Children with autism show atypical preference for non-social stimuli. *Sci. Rep.* **9**, 10355 (2019).
50. S. Bentin, T. Allison, A. Puce, E. Perez, G. McCarthy, Electrophysiological studies of face perception in humans. *J. Cogn. Neurosci.* **8**, 551–565 (1996).
51. N. Kanwisher, G. Yovel, The fusiform face area: A cortical region specialized for the perception of faces. *Philos. Trans. R. Soc. Lond. B Biol. Sci.* **361**, 2109–2128 (2006).
52. J. Orczyk, C. E. Schroeder, I. Y. Abeles, M. Gomez-Ramirez, P. D. Butler, Y. Kajikawa, Comparison of scalp ERP to faces in macaques and humans. *Front. Syst. Neurosci.* **15**, 667611 (2021).
53. J. K. Hesse, D. Y. Tsao, The macaque face patch system: A turtle's underbelly for the brain. *Nat. Rev. Neurosci.* **21**, 695–716 (2020).
54. C. M. Hileman, H. Henderson, P. Mundy, L. Newell, M. Jaime, Developmental and individual differences on the P1 and N170 ERP components in children with and without autism. *Dev. Neuropsychol.* **36**, 214–236 (2011).
55. R. W. Shannon, C. J. Patrick, N. C. Venables, S. He, 'Faceness' and affectivity: Evidence for genetic contributions to distinct components of electrocortical response to human faces. *Neuroimage* **83**, 609–615 (2013).
56. B. Duchaine, L. Germine, K. Nakayama, Family resemblance: Ten family members with prosopagnosia and within-class object agnosia. *Cogn. Neuropsychol.* **24**, 419–430 (2007).
57. A. Johnen, S. C. Schmukle, J. Hüttenbrink, C. Kischka, I. Kennerknecht, C. Dobel, A family at risk: Congenital prosopagnosia, poor face recognition and visuoperceptual deficits within one family. *Neuropsychologia* **58**, 52–63 (2014).
58. M. S. Strauss, L. C. Newell, C. A. Best, S. F. Hannigen, H. Z. Gastgeb, J. L. Giovannelli, The development of facial gender categorization in individuals with and without autism: The impact of typicality. *J. Autism Dev. Disord.* **42**, 1847–1855 (2012).
59. S. Van der Donck, M. Dzhelyova, S. Vettori, S. S. Mahdi, P. Claes, J. Steyaert, B. Boets, Rapid neural categorization of angry and fearful faces is specifically impaired in boys with autism spectrum disorder. *J. Child Psychol. Psychiatry* **61**, 1019–1029 (2020).
60. A. Racca, E. Amadei, S. Ligout, K. Guo, K. Meints, D. Mills, Discrimination of human and dog faces and inversion responses in domestic dogs (*Canis familiaris*). *Anim. Cogn.* **13**, 525–533 (2010).
61. W. A. Freiwald, D. Y. Tsao, M. S. Livingstone, A face feature space in the macaque temporal lobe. *Nat. Neurosci.* **12**, 1187–1196 (2009).
62. D. Y. Tsao, W. A. Freiwald, R. B. Tootell, M. S. Livingstone, A cortical region consisting entirely of face-selective cells. *Science* **311**, 670–674 (2006).
63. N. Strohminger, K. Gray, V. Chituc, J. Heffner, C. Schein, T. B. Heagins, The MR2: A multi-racial, mega-resolution database of facial stimuli. *Behav. Res. Methods* **48**, 1197–1204 (2016).
64. N. J. Sasson, E. W. Touchstone, Visual attention to competing social and object images by preschool children with autism spectrum disorder. *J. Autism Dev. Disord.* **44**, 584–592 (2014).
65. W. Su, T. K. Lam, Z. Yi, N. Ahemaitijiang, Z. R. Han, Q. Wang, Dynamic patterns of affect-biased attention in children and its relationship with parenting. *Int. J. Behav. Dev.* **48**, 25–36 (2024).
66. Y. Zheng, S. Mei, Neural dissociation between reward and salience prediction errors through the lens of optimistic bias. *Hum. Brain Mapp.* **44**, 4545–4560 (2023).

Acknowledgments: We thank S. Mei and Y. Deng for help with data analyses. We also thank A. Miklosi and M. Poo for helpful comments on the manuscript. **Funding:** This work was supported by the National Key Research and Development Program (2021ZD0203901 to Y.Q.Z. and 2019YFA0707103 to S.H.), the National Science Foundation of China (32230043 and 32371092 to S.H. and 32394030 to Y.Q.Z.), the Spring City Plan (2022SCP001 to Y.Q.Z.), and the Wuhan Municipal Project (grant no. 2024020702030125 to Y.Q.Z.). **Author contributions:** Conceptualization: S.Y., Y.Q.Z., and S.H. Methodology: S.Y., C.P., L.W., L.Y., K.G., and S.H. Investigation: S.Y., C.P., and S.H. Visualization: S.Y., Y.Q.Z., and S.H. Supervision: K.G., Y.-h.J., Y.Q.Z., and S.H. Writing—original draft: S.Y., Y.Q.Z., and S.H. Writing—review and editing: S.Y., L.W., K.G., Y.-h.J., Y.Q.Z., and S.H. Funding acquisition: Y.Q.Z. and S.H. Resources: Y.Q.Z. and S.H. Data curation: S.Y. and S.H. Validation: S.Y. and S.H. Formal analysis: S.Y., L.W., Y.Q.Z., and S.H. Software: S.Y. Projection administration: Y.Q.Z. and S.H. **Competing interests:** The authors declare that they have no competing interests. **Data and materials availability:** The data for this study have been deposited in the Data Dryad database (doi: 10.5061/dryad.ht76hdrsp). All data needed to evaluate the conclusions in the paper are present in the paper and/or the Supplementary Materials.

Submitted 6 November 2024
Accepted 26 February 2025
Published 2 April 2025
10.1126/sciadv.adu3793